

Achieving Fixed-Frequency Beam Scanning with a Microstrip Leaky-Wave Antenna Using Double Gaps Capacitor Technique

Mowafak K. Mohsen, *Student Member, IEEE*, M.S.M Isa, A.A.M. Isa, M. K. Abdulhameed, Mothana L. Attiah, *Student Member, IEEE*

Abstract— This study presents a novel half-width microstrip leaky wave antenna (HW-MLWA) that can electronically control main beam at a fixed frequency by using a double-gaps capacitor with diodes, resulting in good impedance matching with small variation gain while scanning. The elementary building blocks of this antenna are periodic HW-MLWA and seven control unit cells (CUCs). A reconfigurable CUC is created by combining two triangle patches as double-gaps capacitor with two diodes as switches to connect the patches with the ground plane. A gap capacitor in each patch cell is independently disconnected or connected by using a PIN diode switch. The reactance profile at the free edge of the microstrip is modified when the state of the patch cell changes, which in turn, shifts the main beam direction. A single-pole double-throw switch is used to achieve backward-to-forward beam scanning at a certain frequency. An HW-MLWA is designed, fabricated, and validated. The proposed antenna prototype can scan the main beam forward between $+28^\circ$ and $+67^\circ$ and backward between -27° and -66° at 4.2 GHz. The measured peak gain of the antenna is 11.12 dBi at 4.2 GHz, the gain variation is 1.3 dB while scanning.

Index Terms— LWA, HW-MLWA, beam scanning, control cell, and gap capacitor

I. INTRODUCTION

Several types of leaky wave antennas (LWAs) have been utilized in scanning beams [1], [2]. Most of uniform and periodic unidirectional LWAs scan the beam in the forward direction only [3]. For instance, the researchers in [4] suggested beam steering of a microstrip line with transverse slots to improve radiation on the endfire. The butterfly substrate-integrated waveguide (SIW) LWA proposed in [5] can control the radiation pattern in the forward direction. The authors in [6] used an SIW-based LWA, which is a forward beam scanning antenna, to radiate from a slot in the broadside. However, some of the LWA showed the tendency to scan in the backward direction, provided some appropriate design variations are employed e.g. use of double-negative meta-materials [7], U-slot [8], ramp-shaped slots [9] etc. Other periodic LWAs offer multiband operation and can also scan the main beam in backward-to-forward directions, but these LWAs cannot scan the beam through the broadside without significant gain losses [10].

A considerable amount of research has been conducted on half-width LWAs with the majority of these studies focusing on scanning in the forward direction. Only a few studies have been

carried out on achieving electronic beam scanning in the backward-to-forward direction with small variation gain while scanning. In [11], the authors presented a novel design with a feeding configuration, and the main beam could scan between 50° and 80° in the forward direction only. Experiments have been conducted on various types of unidirectional periodic LWAs to create continuous beam steering in the backward-to-forward direction, including the broadside. Some periodic half-width microstrip LWAs (HW-MLWAs) could create continuous backward-to-forward beam scanning by altering the placement of shorting vias [12], [13]. Studies have focused on designing an antenna with backward-to-forward beam scanning qualities. In [14], an LWA with backfire-to-endfire scanning capability was developed. In this antenna, the phase constant increased from negative to positive values with the increase in frequency. Hence, the main lobe was scanned in the backward-to-forward direction. In [15], a new design of periodic HW-MLWA was suggested to achieve digital beam scanning by using PIN diode switches, and the scanning range was between 31° and 60° at 6 GHz in the forward direction. The authors in [16] proposed a new reconfigurable design based on SIW-LWA to control the radiation pattern by changing the effective length of SIW, and the scanning range was between 46° and 68° in the forward direction only.

In this letter, a novel technique was developed to scan the radiation pattern at a fixed frequency with small variation in the realized gain for an HW-MLWA. The new HW-MLWA with controlling switch could scan the beam from the backward-to-forward direction by using a double-gaps capacitor with two bias voltage values, which were required to turn the switches on and off. Thus, an easily fabricated and simple single-layer antenna was developed. A HW-MLWA possessed a control unit cell (CUC) configuration that could be redone because it could switch between two states. For the systematic analysis, the antenna design was fabricated and tested. The prototype utilized seven CUCs.

II. ANTENNA CONFIGURATION

The proposed periodic HW-MLWA is shown in [Fig. 1(a), (b), (c), and (d)], which illustrate the top view, feed line, CUC, and Photograph of the fabricated prototype HW-MLWA, respectively. The proposed antenna uses a Rogers RT5880 substrate with length L of 217 mm ($3.039 \lambda_0$), width W of 40 mm ($0.56 \lambda_0$), height h of 1.575 mm, permittivity ϵ_r of 2.2, and $\tan \delta = 0.0009$, where λ_0 is free space wavelength at 4.2 GHz.

The ground plane dimension is the same with the substrate dimension, and the length l_p and width w_p of the microstrip radiating element are 199 mm ($2.787 \lambda_0$) and 11.7 mm ($0.163 \lambda_0$), respectively. The one edge of the HW-MLWA radiating element is connected to the ground plane by a perfect electric wall is carried out by an array of vias, as shown in [Fig. 1(a)]. A septum is used to support the propagation of first high-order mode to avoid the propagation of fundamental TEM wave [17], [18]. The electric wall of the antenna is constructed using 131 pins vias, where the distance between the center to center via is $D_v = 1.5$ mm, and all vias have a diameter of $d_v = 0.8$ mm, see [Fig. 1(b)]. The proposed HW-MLWA is fed from one end, and the other end of the antenna is terminated by a 50Ω to suppress any reflected wave [19], [20]. The dimensions of the SMA connectors are based on commercial dimensions. The gap between the edge of the microstrip line end and the center of first via r is important to force the wave toward the microstrip edges. A tapered feed port is used to improve the matching impedance of the proposed antenna. The dimensions of the tapered feed line w_{f1} and w_{f2} are determined by using the equations in [21], and the length of the tapered line l_f is determined by using the equations in [22]. Furthermore, a parametric study is conducted in the software package CST Microwave Studio for optimization. The length l_f of the tapered line is 10 mm. The width w_{f1} at the end of the microstrip patch line and width w_{f2} of the tapered line are 2 mm and 10.5 mm, respectively.

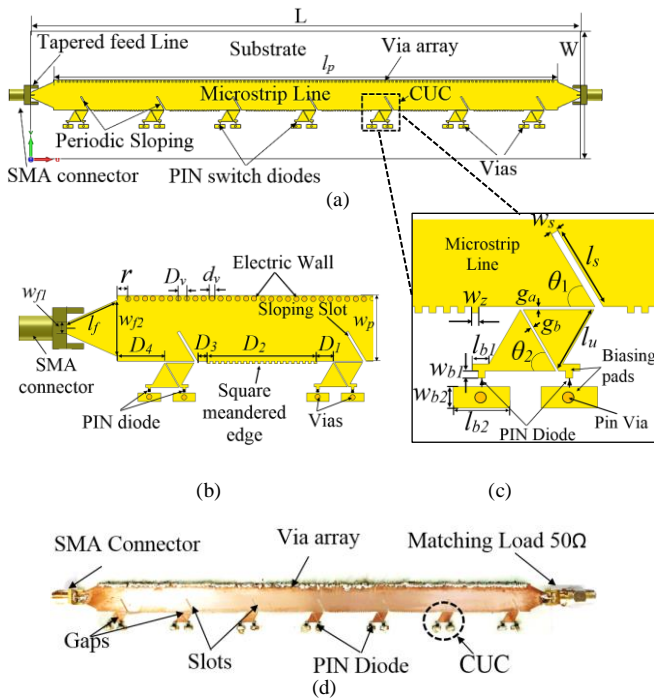


Fig. 1. Reconfigurable HW-MLWA: (a) Top view with periodic slots, (b) Square meandered edge and feed part and (c) Sloping slot. (d) Photograph of the fabricated prototype HW-MLWA.

A. CUC configuration

The researchers in [23] introduced a nonreconfigurable design and reported that large cells after fabrication could not be operated for other configurations. In the present study, the

concept of a reconfigurable CUC is presented. The free edge of the HW-MLWA contains seven equally spaced CUCs with a Space dimensions separation between two cells D_1 , D_2 , and D_3 are of 3 mm, 20 mm, and 2 mm, respectively. The space between the first CUC with the left edge of the microstrip line D_4 is equal to 8.5 mm. Each CUC contains two equilateral triangle patches, PIN diodes as binary switches, and two vias to connect the patches with the ground plane. These patches make double-gap capacitors (first gap between the edge of a microstrip line with triangle patch g_a and the other gap between the patches of two triangles g_b), and the value of these gaps is equal to 0.2 mm. The rib length for each triangle is l_u (5 mm), as shown in [Fig. 1(c)]. The p-terminal of the PIN diode is connected with the triangular patch plane, and the n-terminal is connected to a via. Each via is independently connected with the ground plane by the switch. The patch is isolated to the ground when a diode is in OFF state, that is, reverse biasing, whereas the patch is connected to the ground plane when the diode is in the ON state, that is, forward bias. The total input impedance of the antenna when the PIN diodes are ON can be calculated as [24]. The dimensions of biasing pads l_{b1} , w_{b1} , l_{b2} , and w_{b2} are 1, 0.5, 4, and 1.5, respectively. The dimensions of the new slot were optimized to obtain good matching and radiation. The dimensions of the sloping slot are $l_s \times w_s$ (6 mm \times 0.5 mm), where l_s and w_s are the length and width of the sloping slot, respectively. The sloping angle θ_1 is equal to 60° in order to become the periodic slot are parallel with the CUCs slots (slot between two triangle patches) to avoid any cross-polarization between CUC and radiation element, that's mean θ_1 is should equal to θ_2 .

B. Mathematical analysis of CUCs

The proposed HW-MLWA configuration consists of a microstrip line, gaps, and a seven CUCs. The edge of the microstrip line is considered as a real open circuit having a scattering field, see Fig. 2.

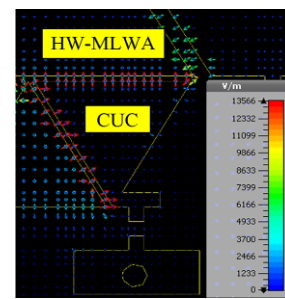


Fig. 2. The electric field between HW-MLWA and CUC.

The microstrip transmission line was shown longitudinally homogeneous by matching the input impedance of the circuit with the terminal capacitance C_t [25]. The relationship between the characteristic impedance Z_c of HW-MLWA with C_t is given by the equation

$$C_t = \Delta_{il} \frac{\epsilon_{eff}}{Z_c c} \quad (1)$$

where c is the velocity of light, ϵ_{eff} the effective dielectric constant and Δ_{il} the conductor extension length; and where

$$\Delta_{il} = A * C * \left(\frac{\epsilon}{D}\right) * h \quad (2)$$

where h is the Rogers RT5880 substrate thickness, $\epsilon_r = 2.2$

$$A = \frac{0.4349 * \left(\left(\epsilon_{eff}^{0.81} + 0.26 \right) \left(\frac{w_p}{h} \right)^{0.8554} + 0.236 \right)}{\left(\epsilon_{eff}^{0.81} - 0.189 \right) \left(\frac{w_p}{h} \right)^{0.8554} + 0.87} \quad (3)$$

$$B = 1 + \frac{\left(\frac{w_p}{h} \right)^{0.371}}{(2.358\epsilon_r + 1)} \quad (4)$$

$$C = 1 + \left(\frac{0.5274}{\epsilon_{eff}^{0.9236}} \right) \tan^{-1} \left[0.084 \left(\frac{w_p}{h} \right)^{1.943/B} \right] \quad (5)$$

$$D = 1 + 0.0377 \left[6 - 5e^{(0.036(1-\epsilon_r))} \right] + \tan^{-1} \left[0.067 \left(\frac{w_p}{h} \right)^{1.456} \right] \quad (6)$$

$$E = 1 - 0.218e^{\left[-7.5 \frac{w_p}{h} \right]} \quad (7)$$

According to Fig. 3, the equivalent circuit of the gap capacitor as π -circuit consists of gap coupling C_{ga} and capacitances of plate C_{ga1} and C_{ga2} . [26].

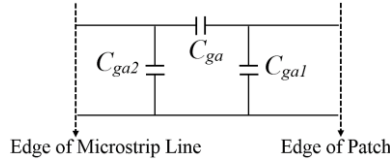


Fig. 3. The equivalent circuit for the gap capacitor.

The accurate equations for plate capacitances C_{ga1} and C_{ga2} and coupling capacitance C_{ga} of the equivalent circuit of the gap capacitance are derived from the hybrid mode analysis [27] The equations are

$$C_{ga} = 0.5 * Q_1 * h * e^{\left(-1.86 * \frac{Q_2}{h} \right)} * \left[1 + 4.19 * \left\{ 1 - e^{\left(0.785 * \sqrt{h/w_p} * l_u/w_p \right)} \right\} \right] \quad (8)$$

$$C_{ga2} = C_{t2} * \left[\frac{Q_2 + Q_3}{Q_2 + 1} \right]; \quad C_{ga1} = C_{t1} * \left[\frac{Q_2 + Q_4}{Q_2 + 1} \right] \quad (9)$$

Where

$$Q_1 = 0.04598 \left\{ 0.03 + \left(\frac{w_p}{h} \right)^{Q_5} \right\} (0.272 + \epsilon_r * 0.07) \quad (10)$$

$$Q_2 = 0.107 \left(\frac{w_p}{h} + 9 \right) \left(l_u/h \right)^{3.23} + 2.09 \left(l_u/h \right)^{1.05} \left[\frac{1.5 + 0.3 \left(\frac{w_p}{h} \right)}{1 + 0.6 \left(\frac{w_p}{h} \right)} \right] \quad (11)$$

$$Q_3 = e^{\left[-0.5978 \left(\frac{w_p}{l_u} \right)^{1.35} \right] - 0.55} \quad (12)$$

$$Q_4 = e^{\left[-0.5978 \left(\frac{w_p}{l_u} \right)^{1.35} \right] - 0.55} \quad (13)$$

$$Q_5 = \frac{1.23}{\left[1 + 0.12 \left(\left(\frac{l_u}{w_p} \right) - 1 \right)^{0.9} \right]} \quad (14)$$

As shown in Eq. (8), the permittivity of the substrate is important in selecting good impedance for the feed line to obtain maximum radiation and good matching. In this design, ϵ_r is 2.2 for the Rogers RT5880 substrate. [Fig. 4(a)] shows the relationship between the gap capacitance C_{ga} with gap length L_u , because the equivalent capacitance across the tank circuit increases with the gap length. Hence, the gap capacitor between the CUC and microstrip line has important roles in the control radiation pattern. This can be attributed to the fact that the coupling between two patches are ineffective when the air gap lengths are large, that's very clear in [Fig. 4(b)]. In fact, coupling capacitance C_{ga} decreases and terminal capacitance increases with gap length. Thus, the impedance of the antenna with the gap coupled for CUCs plays a significant role in controlling frequency. Such that the input impedance increases

with the increase of frequency that leads to change the reactance profile of the antenna which changes the propagation constant and eventually causes a change in the main beam direction.

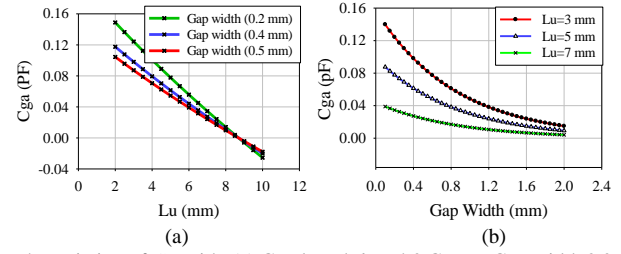


Fig. 4. Variation of C_{ga} with: (a) Gap length l_u at 4.2 GHz at Gap width 0.2 mm, 0.4 mm, and 0.5 mm. (b) Gap width at 4.2 GHz at $L_u = 3$ mm, 5 mm, and 7 mm.

III. RESULT AND MEASUREMENT

To prove the concept for the present antennas, the design was fabricated and tested. Fig. 5 illustrates that each end of the proposed antenna is provided by a simple feed network. The simple feed network consists of a coaxial feed cable, two parallel branches with EV1HMC8038LP4C controlling switches based on the data sheet [28], and a single-pole double-throw (SPDT) switch in a leadless surface mount package, which had high isolation and was nonreflective from 0.1 GHz to 6.0 GHz. This switch was ideal for cellular infrastructure applications that yield up to 62 dB isolation at 4.0 GHz, 0.8 dB insertion loss at 4.0 GHz with 60 dBm input third-order intercept. SPDT had three ports and operated under one operation mode with the control circuit acting as the switch. The two ports in HW-MLWA were regulated by the EV1HMC8038LP4C controlling switch. Table I presents the predicted and measured scanning ranges in the backward and forward directions for five different CUCs when the connections of the feed and load change. For beam scanning in the forward region, ports 1 and 2 were connected to the RF signal and matching load of 50 Ω , respectively. For beam scanning in the backward region, ports 2 and 1 were connected to the RF signal and matching load, respectively. Fig. 6 illustrates the backward to forward radiation patterns of the proposed HW-MLWA, in which the forward scanning ranges between $+24^\circ$ and $+63^\circ$ and the backward scanning ranges between -24° and -63° .

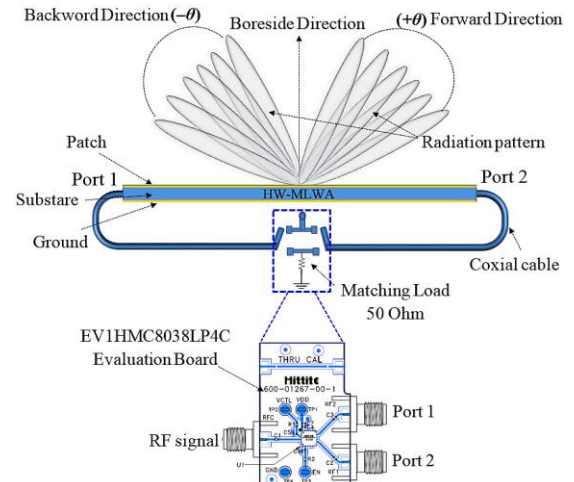


Fig. 5. Proposed antenna with backward to forward beam scanning.

TABLE I

SELECTED SWITCH CASES AND DIRECTION OF THE MAIN BEAM AT 4.2 GHz

State NO.	CUC state	*FW		**BW		Realized gain (dBi)	
		P	M	P	M	P	M
1	00-00-00-00-00-00-00	+24°	+28°	-24°	-27°	11.3	11.1
2	11-00-11-00-11-00-11	+31°	+35°	-31°	-35°	11.2	11
3	10-10-10-10-10-10-10	+37°	+37°	-37°	-41°	11.1	10.9
4	01-01-01-01-01-01-01	+53°	+53°	-53°	-57°	10.9	10.7
5	11-11-11-11-11-11-11	+63°	+67°	-63°	-66°	9.9	9.8

*FW (Forward direction) at port1 connect to RF signal and port 2 connect to matching load.

**BW (Backward direction) at port2 connect to RF signal and port 1 connect to matching load); P: predict; M: measured

The S-parameters of the prototype were measured by using an Agilent E5071C network analyzer. [Fig. 7(a)] shows the measured and predicted input reflection coefficient magnitudes for states 1 and 5 CUCs. The measured and predicted results were consistent. However, a slight difference was observed between the predicted and measured S-parameters due to the tangent loss of the substrate and fabrication tolerance. The level of S_{11} is lower than -10dB for all the five states at 4.2 GHz.

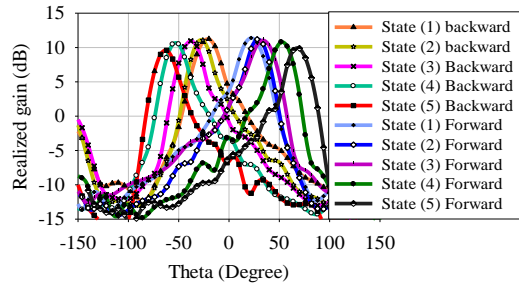


Fig. 6. Radiation patterns (x-z plane) in a backward to forward direction at 4.2 GHz for different switching configurations in Table I.

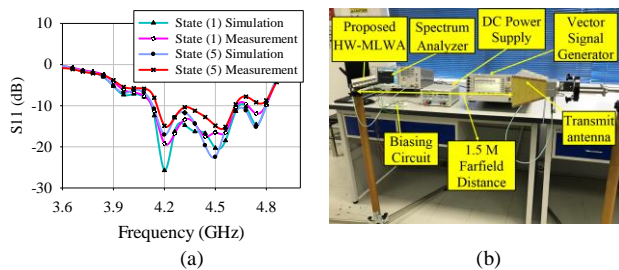


Fig. 7. (a) Simulation and measurement of the reflection coefficient for states (1) and (5) for backward to forward direction. (b) Comparison-method to measure the gain.

The gain-comparison method was used to measure the gain at 4.2 GHz for five selective switches (in Table I) by using the transmit horn antenna [Fig. 7(b)]. The distance of the far-field between the reference and proposed antennas is equal to ~ 1.5 m. The gain variation during backward and forward scanning is 1.3 dB only. The radiation characteristics were measured in UTeM university. Fig. 8 shows that the proposed HW-MLWA is polarized in the x-direction and horizontally placed to align with the reference antenna. Fig. 9 presents the radiation pattern measurement of the proposed HW-MLWA in the x-z plane. A

similar trend was observed between the measured and simulation results with a small margin at approximately 3° to 4° . The measured radiation pattern in the forward direction with the change in CUCs could be steered in discrete steps between $+28^\circ$ in state 1 and $+67^\circ$ in state 5. The measured radiation pattern in the backward direction could be steered in discrete steps between -27° in state 1 and -66° in state 5 at 4.2 GHz.

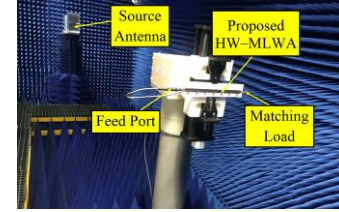


Fig. 8. Pattern measurement setup at the UTeM university.

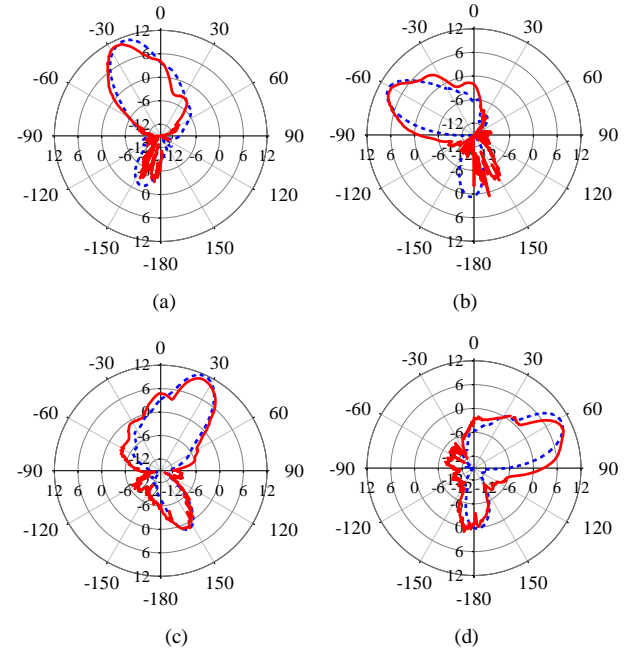


Fig. 9. Predict (blue dash-line) and Measured (red line) radiation patterns of the reconfigurable HW-MLWA on the x-z plane (H-plane) at 4.2 GHz. (a) State 1 backward. (b) State 5 backward. (c) State 1 forward. (d) State 5 forward (Phi=0).

IV. CONCLUSION

This study presents a new double-gap capacitor technique to control the radiation of periodic HW-MLWAs at a fixed frequency. The reconfigurable CUC contains two triangular patches with two PIN diodes. The free edge of the microstrip line is loaded with periodic double-gap capacitors, and PIN diodes are used to control their connections with the ground plane. The proposed design aids in achieving backward-to-forward beam scanning with small variation gain. A multistate control cell approach is developed to analyze reconfigurable periodic structures, and this approach is used to design reconfigurable MLWAs. The proposed methodology is valuable for the systematic analysis of periodic structures. The measured scanning range of the designed antenna is 38° and 39° in the backward and forward directions with gain variation while scanning at 1.3 dB, respectively. The measured peak gain at 4.2 GHz is 11.12 dBi. The design is suitable for the C-band applications.

REFERENCES

- [1] Q. Lai, C. Fumeaux, and W. Hong, "Periodic leaky-wave antennas fed by a modified half-mode substrate integrated waveguide," *IEEE Microwaves, Antennas Propag.*, vol. 6, no. 5, pp. 594–601, 2012.
- [2] S. K. Podilchak, L. Matekovits, A. P. Freundorfer, Y. M. M. Antar, and M. Orefice, "Controlled Leaky-Wave Radiation From a Planar Configuration of Width-Modulated Microstrip Lines," *IEEE Trans. Antennas Propag.*, vol. 61, no. 10, pp. 4957–4972, 2013.
- [3] D. K. Karmokar, Y. J. Guo, P. Qin, S. Chen, and T. S. Bird, "Substrate Integrated Waveguide-Based Periodic Backward-to-Forward Scanning Leaky-Wave Antenna With Low Cross-Polarization," *IEEE Trans. Antennas Propag.*, vol. 66, no. 8, pp. 3846–3856, 2018.
- [4] J. Liu, D. R. Jackson, and Y. Long, "Substrate integrated waveguide (SIW) leaky-wave antenna with transverse slots," *IEEE Trans. Antennas Propag.*, vol. 60, no. 1, pp. 20–29, 2012.
- [5] Y. Mohtashami and J. Rashed-Mohassel, "A butterfly substrate integrated waveguide leaky-wave antenna," *IEEE Trans. Antennas Propag.*, vol. 62, no. 6, pp. 3384–3388, 2014.
- [6] P. Lorenz and M. Sa, "A Substrate Integrated Waveguide Leaky Wave Antenna Radiating from a Slot in the Broad Wall," in *IEEE MTT-S International Microwave Symposium digest. IEEE MTT-S International Microwave Symposium · June 2010*, 2010, no. June, pp. 5–8.
- [7] I. T. M. Supercells, A. Mehdipour, and G. V. Eleftheriades, "Leaky-Wave Antennas Using Negative-Refractive- Index Transmission-Line Metamaterial Supercells," *IEEE Trans. Antennas Propag.*, vol. 62, no. 8, pp. 3929–3942, 2014.
- [8] D. K. Karmokar and K. P. Esselle, "Periodic U-Slot-Loaded Dual-Band Half-Width Microstrip Leaky-Wave Antennas for Forward and Backward Beam Scanning," *IEEE Trans. Antennas Propag.*, vol. 63, no. 12, pp. 5372–5381, Dec. 2015.
- [9] A. P. Saghati, S. Member, and M. M. Mirsalehi, "A HMSIW Circularly Polarized Leaky-Wave Antenna With Backward , Broadside , and Forward Radiation," *IEEE Antennas Wirel. Propag. Lett.*, vol. 13, pp. 451–454, 2014.
- [10] D. K. Karmokar, Y. J. Guo, P. Qin, K. P. Esselle, T. S. Bird, and L. Fellow, "Forward and Backward Beam-Scanning Tri-Band Leaky-Wave Antenna," *IEEE Antennas Wirel. Propag. Lett.*, vol. 16, pp. 1891–1894, 2017.
- [11] Y. Li and Y. Long, "Frequency-fixed beam-scanning microstrip leaky-wave antenna with multi-terminals," *Electron. Lett.*, vol. 42, no. 1, pp. 4–5, 2006.
- [12] Y. Li, Q. Xue, E. K. N. Yung, and Y. Long, "The periodic half-width microstrip leaky-wave antenna with a backward to forward scanning capability," *IEEE Trans. Antennas Propag.*, vol. 58, no. 3, pp. 963–966, 2010.
- [13] Y. Li, Q. Xue, H. Tan, and Y. Long, "The Half-Width Microstrip Leaky Wave Antenna With the Periodic Short Circuits," *IEEE Trans. Antennas Propag.*, vol. 59, no. 9, pp. 3421–3423, 2011.
- [14] L. Liu, C. Calos and T. Itoh, "Dominant mode leaky-wave antenna with backfire-to-endfire scanning capability," *Electron. Lett.*, vol. 38, no. 23, pp. 1414–1416, 2002.
- [15] D. K. Karmokar, K. P. Esselle, and S. G. Hay, "Fixed-Frequency Beam Steering of Microstrip Leaky-Wave Antennas Using Binary Switches," *IEEE Trans. Antennas Propag.*, vol. 64, no. 6, pp. 2146–2154, Jun. 2016.
- [16] Y. Geng, J. Wang, Y. Li, Z. Li, M. Chen, and Z. Zhang, "Radiation Pattern-Reconfigurable Leaky-Wave Antenna for Fixed-Frequency Beam Steering Based on Substrate-Integrated Waveguide," *IEEE Antennas Wirel. Propag. Lett.*, vol. 18, no. 2, pp. 387–391, 2019.
- [17] M. J. H. and A. J. T. A. G. M. Zelinski, G. A. Thiele, M. L. Hastriter, "Half width leaky wave antennas," *Eur. Sp. Agency, (Special Publ. ESA SP*, vol. 626 SP, pp. 341–348, 2007.
- [18] D. K. Karmokar, D. N. P. Thalakituna, K. P. Esselle, L. Matekovits, and M. Heimlich, "Reconfigurable half-width microstrip leaky-wave antenna for fixed-frequency beam scanning," in *2013 7th European Conference on Antennas and Propagation, EuCAP 2013*, 2013, pp. 1314–1317.
- [19] D. K. Karmokar, K. P. Esselle, D. N. P. Thalakituna, M. Heimlich, and L. Matekovits, "A leaky-wave antenna for beam steering in forward and backward directions," in *2013 1st IEEE TENCON Spring Conference, TENCONSpring 2013*, 2013, pp. 47–50.
- [20] N. Nguyen-Trong, L. Hall, and C. Fumeaux, "Transmission-Line Model of Nonuniform Leaky-Wave Antennas," *IEEE Trans. Antennas Propag.*, vol. 64, no. 3, pp. 883–893, 2016.
- [21] D. Deslandes, "Design equations for tapered microstrip-to-Substrate Integrated Waveguide transitions," *IEEE MTT-S Int. Microw. Symp. Dig.*, pp. 704–707, 2010.
- [22] K. Lu, "An efficient method for analysis of arbitrary nonuniform transmission lines," *IEEE Trans. Microw. Theory Tech.*, vol. 45, no. 1, pp. 9–14, 1997.
- [23] Z. Ma, L. Jiang, S. Gupta, and W. Sha, "Dispersion Characteristics Analysis of One Dimensional Multiple Periodic Structures and Their Applications to Antennas," *IEEE Trans. Antennas Propag.*, vol. 63, no. 1, pp. 113–121, 2015.
- [24] J. A. Ansari, P. Singh, N. P. Yadav, and B. R. Vishvakarma, "Analysis of Shorting Pin Loaded Half Disk Patch Antenna for Wideband Operation," *Prog. Electromagn. Res. C*, vol. 6, no. January, pp. 179–192, 2009.
- [25] A. Asthana and B. R. Vishvakarma, "Analysis of gap-coupled microstrip antenna," *International Journal of Electronics*, November 2014, pp. 37–41, 2010.
- [26] M. M. Norbert, H. L. Koster, and R. H. Jansen, "The equivalent circuit of asymmetrical series gap in microstrip and suspended substrate lines," *IEEE Trans. Microw. Theory Tech.*, vol. 30, pp. 1273–1279, 1982.
- [27] A. Gopinath, "Parameters of Discontinuities Microstriplines," *IEEE Trans. Microw. Theory Tech.*, vol. 26, pp. 831–836, 1978.
- [28] Analog Devices. *HMC8038 SPDT* [online]. available : https://my.mouser.com/datasheet/2/307/2SMES-01_0911-15621.pdf, 2015.